Supporting Infomration for: Metadynamics Investigation of Lanthanide Solvation Free Energy Landscapes and Insights into Separations Energetics

Xiaoyu Wang,*,† Allison A. Peroutka,‡ Dmytro V. Kravchuk,† Jenifer C. Shafer,‡ Richard E. Wilson,† and Michael J. Servis*,†

†*Chemical Sciences and Engineering Division, Argonne National Laboratory, 9700 S Cass Ave, Lemont, IL 60439*

‡*Department of Chemistry, Colorado School of Mines, 1500 Illinois St., Golden, CO, 80401, USA*

E-mail: xiaoyu.wang@anl.gov; mservis@anl.gov

Materials

The DMDOHEMA extractant was synthesized and purchased from Technocomm Ltd. with a purity of 99% by HPLC. La(III) nitrate hexahydrate, Eu(III) nitrate pentahydrate, Lu(III) nitrate hydrate, and n-dodecane were obtained from Sigma-Aldrich. Optima grade nitric acid (HNO3) was obtained from Fisher Scientific. All chemicals are used as received.

Solvent Extraction

Solvent extraction experiments are performed to separate rare earth metal ions from the aqueous phase to the organic phase. The aqueous phase is prepared by directly desolving the rare earth nitrate salts in 10 mM HNO_3 with 3M $LiNO_3$ solution. The presence of HNO_3 prevents hydrolysis induced by heavy lanthanides. The use of $LiNO_3$ instead of HNO_3 provides the sufficient anion source to drive the separation through the solvation mechanism. Different from trivalent lanthanide ions, the metal-ligand binding energy for the monovalent Li^+ ion is not sufficient to outcompete its hydration free energy, while prohibits its coextraction with the lanthanide ion. The final samples contain 1mM $La(NO_3)_3$, 1mM $Eu(NO_3)_3$, 1mM $Lu(NO_3)_3$, 3M $LiNO_3$ and 10mM HNO_3 in the aqueous phase. The organic phases are prepared by desolving 6 different amounts of DMDOHEMA extractant in heptane. Therefore, we obtain 6 organic phases with 0.05, 0.1, 0.2, 0.4, 0.8 and 1.0M of DMDOHEMA. A 1.5 mL of the organic phases are first pre-equilibrated with 10 mM HNO_3, 3M $LiNO_3$ solution for 30 min at 2000 rpm and then centrifuged for 5 min at 2800 rpm. A 1.0 mL of the pre-equilibrated organic phase is separated from the top layer, transferred to another clean tube, and mixed with a 1.0 mL rare earths-containing aqueous solution. The sample is then shaken for 60 min at 2000 rpm and then centrifuged for 5 min at 2800 rpm. All extraction experiments are carried out at room temperature, between 20 and 25°C.

ICP-MS

After solvent extraction experiments, rare earth metal concentrations in the organic phase and the aqueous phase under different extraction conditions are measured by an Agilent 7900 inductively coupled plasma mass spectrometry instrument (ICP-MS). All samples are diluted to the range of 50 — 200 ppb by 2wt% HNO_3, where ICP-MS is able to provide accurate measurements. To directly measure the organic phase, the sample is mixed with equal volume of ethanol before dilution with 2wt% HNO_3 solution. After measurement, the ppb values are backcalculated to obtain the original concentrations. To ensure precision, we

also measured the initial concentration of rare earth before solvent extractions. Generally, a mass balance has been achieved within 5%.

Distribution ratio calculation

In SX, the distribution ratio (D) is often used as an indicator to show the separation performance for a specific rare earth element. Shown in Equation (1) (the overbar denotes the composition in the organic phase), D is calculated as the ratio of rare earth concentrations in the organic and aqueous phase by assuming equal volumes of both organic and aqueous phases.

$$D_{Ln} = \frac{\overline{[Ln]}}{[Ln]} \tag{1}$$

The overall extraction reaction of lanthanides by DMDOHEMA can be expressed by Equation (2).

$$[Ln^{3+}] + n\overline{[DMDOHEMA]} + 3[NO_3^-] \Longleftrightarrow \overline{[Ln(DMDOHEMA)_n(NO_3)_3]} \tag{2}$$

Rearranging the equation and using the D in Equation (1) result in Equation (3), in which K_{ex} is the extraction rate constant.

$$logK_{ex} = logD_{Ln} - nlog\overline{[DMDOHEMA]} - 3log[NO_3^-] \tag{3}$$

From there we can see that the overall stoichiometry, n, of the metal-ligand speciation can be derived from the distribution ratio measured in Equation (3). All the D values along with the fitted slopes are shown in Figure S1.

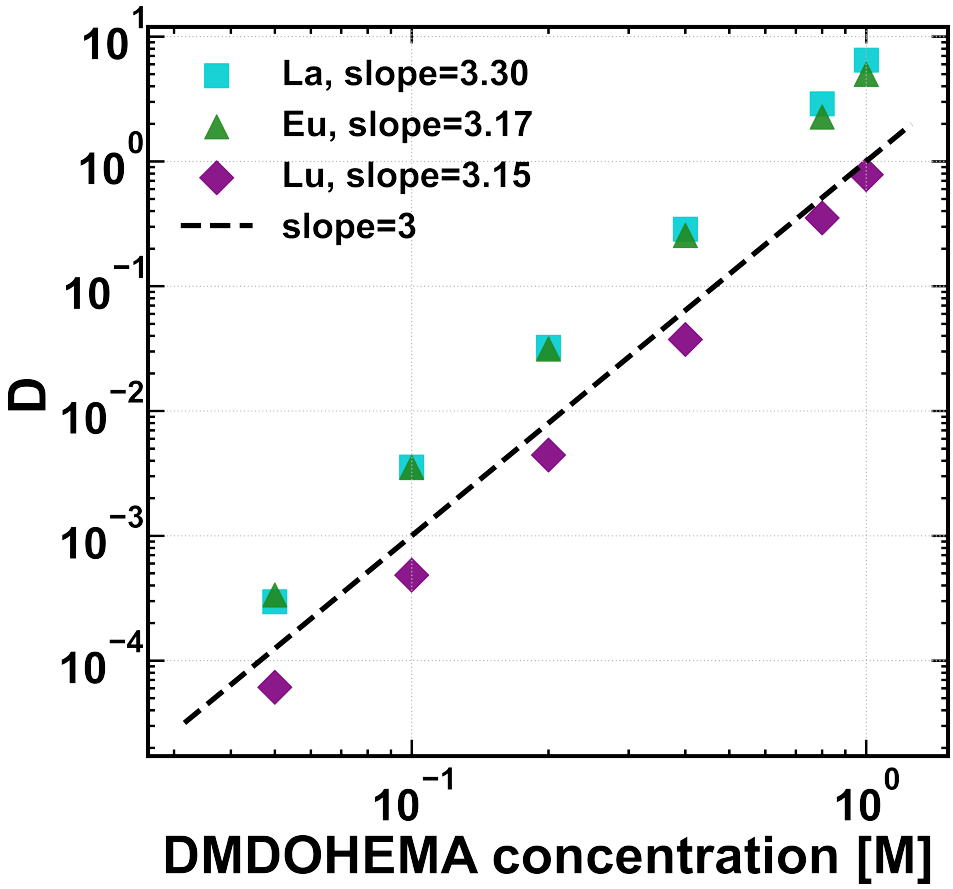

Figure S1: Extractant dependencies for the extraction of La(III), Eu(III) and Lu(III) by MA in n-heptane. Best-fitted slopes are shown in the figure legend.

FTIR

1.5 mL of 0.5M DMDOHEMA in heptane is precontact with 1.5 mL of 3M $LiNO_3$ aqueous solution for 60 minutes. Then 1 mL "pre-equilibrated" organic phase is contact with 1.0 mL aqueous solution containing 25mM $Eu(NO_3)_3$, 3M $LiNO_3$ for 60 minutes. The organic phase with Eu contact and the pre-contact organic phases are then analyzed by FT-IR. ATR-FTIR spectra were collected with a Nicolet iS50 ATR spectrometer equipped with a 2.8 mm round, type IIa diamond crystal, KBr beamsplitter, and a DTGS detector. Spectra were collected with a resolution of 4 cm^{-1}, a zero-filling factor of 2, and 32 scans per spectrum in the wavenumber range of 4000 to 400 cm^{-1}.

TRLIFS

The sample is prepared by adding a 2 mL aliquot of the organic phase after Eu extraction to a quartz fluorescence cuvette. Lifetime measurements are collected with an OPOTEK tunable pulse laser with an excitation of 394 nm, at an emission of 617 nm, and an emission bandwidth of 0.2 nm. During data collection, the solution in the cuvette is stirred at 1200 rpm at a constant temperature of 20°C. To determine the number of coordinating H_2O molecules to Eu (n_{H_2O}), solvent extraction experiments are conducted from both H_2O and D_2O aqueous phases enabling a more accurate determination for the number of coordinating H_2O molecules to Eu. After data collection, lifetime measurements are fit with a single exponential function, where resulting Eu lifetimes for both H_2O and D_2O experiments yielded τ_{H_2O} and τ_{D_2O}, respectively. The corresponding Eu lifetimes are used in Equation (4) to quantify the number of H_2O molecules on the Eu inner coordination sphere.[1,2] Lifetime measurements resulted in τ_{H_2O} of 0.766 ms and τ_{D_2O} of 1.17 ms. Applying these Eu lifetimes to Equation (4) results in 0.14 ± 0.5 H_2O molecules coordinating with Eu. The ± 0.5 error in number of H_2O molecules results from the error in the linear regression between $1/\tau$ and the number of bound H_2O molecules determined from single crystal X-ray diffraction.[2]

$$n_{H_2O} = 1.11 \left[\frac{1}{\tau_{H_2O}} - \frac{1}{\tau_{D_2O}} - 0.31 \right] \tag{4}$$

MD simulations

Equation (5) describes the non-bonded intermolecular interaction used in the 12-6-4 potential.[3–6] C4 terms for rare-earth ions have been reparamterized by Duvail et al., and used in this work. The General AMBER Force Field (GAFF2)[8,9] is used for compounds other than rare-earth ions, including hexane, NO_3^-, and DMDOHEMA. The atomic charges of these molecules are derived using Austin Model 1 with the bond charge correction method (AM1-BCC),[10,11] while BCC charges on the NO_3^- are derived based on He et al.'s work.[9] For the water, we use the four-site OPC model,[12] which is compatible with the rare-earth

ion reparameterization.[7]

$$U_{inter} = \sum_{i,j} \left\{ \frac{1}{4\pi\epsilon} \frac{q_i q_j}{r_{ij}} + \epsilon_{ij} \left[\left(\frac{R^{\min}{}_{ij}}{r_{ij}} \right)^{12} - 2 \left(\frac{R^{\min}{}_{ij}}{r_{ij}} \right)^{6} \right] - \frac{C4_{ij}}{r_{ij}^4} \right\} \tag{5}$$

Initially, a rare-earth ion, bound with 3 DMDOHEMAs in bidentate manner, 3 NO_3^- in the monodentate manner, and 1 water, is packed with 125 hexane molecules using PACKMOL.[13] Topology and force field files are generated by AmberTools 23.[14] MD simulations are carried out in the AMBER software package[15] with PLUMED as the plugin advanced sampling tool.[16] 1 ns equilibration without advanced sampling is performed at 1 atm with a Berendsen barostat[17] and 300 K by the Langevin thermostat.[18,19] The system is then sampled by well-tempred metadynamics[20,21] for 4 μs in an NVT ensemble to produce the free energy landscape. All hydrgon atoms are constraint to other heavy atoms using the SHAKE algorithm.[22,23] 2 fs per MD step is used for all simulations. In the metadynamics, the potential was generated by spawning Gaussian hills every 500 MD step. The height and width of the Gaussians are 0.2 kJ/mol and 0.15 in the 3D coordination number space, with a bias factor of 25 in well-tempered metadynamics to control the height of the adaptive Gaussian potential. After the well-tempered MetaD simulation, the trajectory and bias potentials are reweighted based on an estimator in Tiwary and Parrinello's work.[21] All simulation inputs, inlcuding parameter, topology files, PLUMED run and reweight scripts, are provided on Zenodo (https://zenodo.org/records/13730351).[24]

It is worth clarifying the relationship between stoichiometry and CVs here. While we can experimentally determine reasonable combinations of molecules in the complex, we use the simulation to determine the relative energies of all possible coordination environments given that fixed stoichiometry. The stoichiometry limits the accessible values of the CVs by limiting the possible combinations of coordinating atoms. The CVs operate on distances between atoms, because the overall stoichiometry alone does not uniquely define the possible combinations of denticity for multidentate MA and NO_3 ligands. By allowing any possible combination of coordinating oxygen atoms within the limits defined by the stoichiometry of

the complex, we can determine the entire free energy surface within that CV space.

Convergence tests

In order to make sure that all MetaD simulations have adequately sampled the configurational space, we perform the convergence tests on selective local minima during the last μs of the simulation. The results are shown in Figure S2. From there, we can see that all the favorable local minima are fluctuating around the reference state. Error bars in the main text are generated by take standard deviations of all profiles for the last 2 μs.

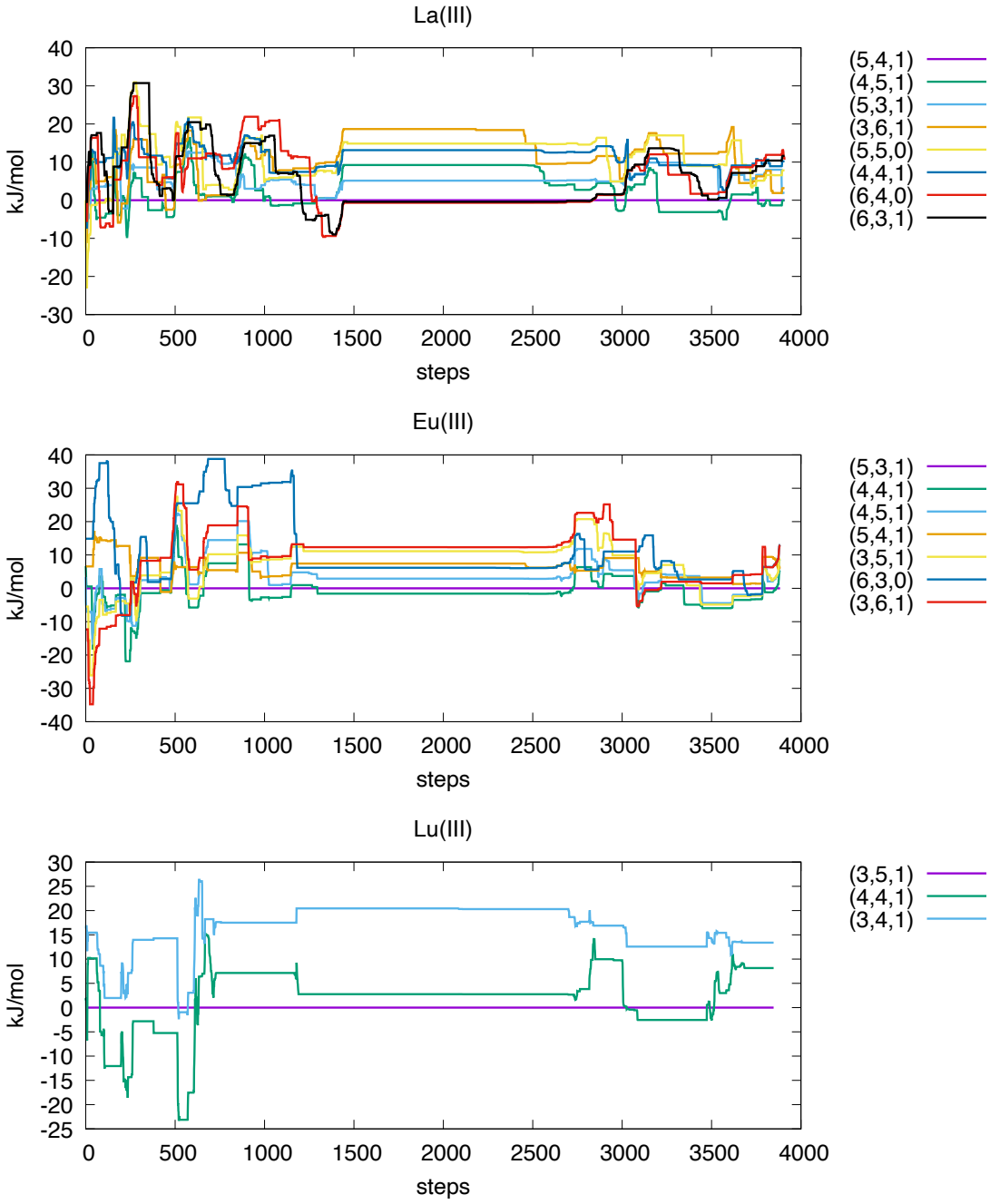

Figure S2: Convergence tests for selective minima during the last μs of the simulation.

References

(1) W. D. Horrocks, J.; Sudnick, D. R. Lanthanide Ion Probes of Structure in Biology. Laser-Induced Luminescence Decay Constants Provide a Direct Measure of the Number

of Metal-Coordinated Water Molecules. *J. Am. Chem. Soc.* **1979**, *101*, 334–340.

(2) Supkowski, R. M.; W. D. Horrocks, J. On the determination of the number of water molecules, q, coordinated to europium(III) ions in solution from luminescence decay lifetimes. *Inorg. Chim. Acta* **2002**, *340*, 44–48.

(3) Li, P.; Merz Jr, K. M. Taking into account the ion-induced dipole interaction in the nonbonded model of ions. *Journal of Chemical Theory and Computation* **2014**, *10*, 289–297.

(4) Li, P.; Song, L. F.; Merz Jr, K. M. Parameterization of highly charged metal ions using the 12-6-4 LJ-type nonbonded model in explicit water. *The Journal of Physical Chemistry B* **2015**, *119*, 883–895.

(5) Li, P.; Song, L. F.; Merz Jr, K. M. Systematic parameterization of monovalent ions employing the nonbonded model. *Journal of Chemical Theory and Computation* **2015**, *11*, 1645–1657.

(6) Li, Z.; Song, L. F.; Li, P.; Merz Jr, K. M. Parametrization of Trivalent and Tetravalent Metal Ions for the OPC3, OPC, TIP3P-FB, and TIP4P-FB Water Models. *Journal of Chemical Theory and Computation* **2021**, *17*, 2342–2354.

(7) Duvail, M.; Moreno Martinez, D.; Ziberna, L.; Guillam, E.; Dufrêche, J.-F.; Guilbaud, P. Modeling Lanthanide Ions in Solution: A Versatile Force Field in Aqueous and Organic Solvents. *Journal of Chemical Theory and Computation* **2024**,

(8) Wang, J.; Wolf, R. M.; Caldwell, J. W.; Kollman, P. A.; Case, D. A. Development and testing of a general amber force field. *Journal of Computational Chemistry* **2004**, *25*, 1157–1174.

(9) He, X.; Man, V. H.; Yang, W.; Lee, T.-S.; Wang, J. A fast and high-quality charge

model for the next generation general AMBER force field. *The Journal of Chemical Physics* **2020**, *153*, 114502.

(10) Jakalian, A.; Bush, B. L.; Jack, D. B.; Bayly, C. I. Fast, efficient generation of high-quality atomic charges. AM1-BCC model: I. Method. *Journal of Computational Chemistry* **2000**, *21*, 132–146.

(11) Jakalian, A.; Jack, D. B.; Bayly, C. I. Fast, efficient generation of high-quality atomic charges. AM1-BCC model: II. Parameterization and validation. *Journal of Computational Chemistry* **2002**, *23*, 1623–1641.

(12) Izadi, S.; Anandakrishnan, R.; Onufriev, A. V. Building water models: a different approach. *The Journal of Physical Chemistry Letters* **2014**, *5*, 3863–3871.

(13) Martínez, L.; Andrade, R.; Birgin, E. G.; Martínez, J. M. PACKMOL: A package for building initial configurations for molecular dynamics simulations. *Journal of Computational Chemistry* **2009**, *30*, 2157–2164.

(14) Case, D. A.; Aktulga, H. M.; Belfon, K.; Cerutti, D. S.; Cisneros, G. A.; Cruzeiro, V. W. D.; Forouzesh, N.; Giese, T. J.; Gotz, A. W.; Gohlke, H.; others AmberTools. *Journal of Chemical Information and Modeling* **2023**, *63*, 6183–6191.

(15) Case, D. et al. Amber. 2023; University of California, San Francisco.

(16) Tribello, G. A.; Bonomi, M.; Branduardi, D.; Camilloni, C.; Bussi, G. PLUMED 2: New feathers for an old bird. *Computer Physics Communications* **2014**, *185*, 604–613.

(17) Berendsen, H. J.; Postma, J. v.; Van Gunsteren, W. F.; DiNola, A.; Haak, J. R. Molecular dynamics with coupling to an external bath. *The Journal of Chemical Physics* **1984**, *81*, 3684–3690.

(18) Uberuaga, B. P.; Anghel, M.; Voter, A. F. Synchronization of trajectories in canonical molecular-dynamics simulations: Observation, explanation, and exploitation. *The Journal of Chemical Physics* **2004**, *120*, 6363–6374.

(19) Sindhikara, D. J.; Kim, S.; Voter, A. F.; Roitberg, A. E. Bad seeds sprout perilous dynamics: Stochastic thermostat induced trajectory synchronization in biomolecules. *Journal of Chemical Theory and Computation* **2009**, *5*, 1624–1631.

(20) Barducci, A.; Bussi, G.; Parrinello, M. Well-tempered metadynamics: a smoothly converging and tunable free-energy method. *Physical Review Letters* **2008**, *100*, 020603.

(21) Tiwary, P.; Parrinello, M. A time-independent free energy estimator for metadynamics. *The Journal of Physical Chemistry B* **2015**, *119*, 736–742.

(22) Ryckaert, J.-P.; Ciccotti, G.; Berendsen, H. J. Numerical integration of the cartesian equations of motion of a system with constraints: molecular dynamics of n-alkanes. *Journal of Computational Physics* **1977**, *23*, 327–341.

(23) Miyamoto, S.; Kollman, P. A. Settle: An analytical version of the SHAKE and RATTLE algorithm for rigid water models. *Journal of Computational Chemistry* **1992**, *13*, 952–962.

(24) Wang, X. Insights into Rare Earth Solvation Energetics in the Organic Phase and Understanding its Impacts on the Separation Performance. 2024; https://doi.org/10.5281/zenodo.13730351.